Nanoscale

Accepted Manuscript

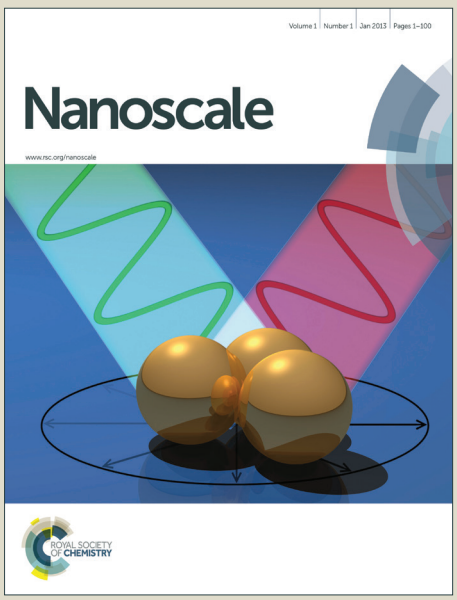

ROYAL SOCIETY OF CHEMISTRY

www.rsc.org/nanoscale

Nanoscale

RSCPublishing

COMMUNICATION

Cite this: DOI: 10.1039/xoxxoooooox

Insights into the effect of nanoconfinement on molecular interactions†

Received ooth January 2014,
Accepted ooth January 2014

DOI: 10.1039/xoxxoooooox

www.rsc.org/nanoscale

Yang Chen[a], Shuangshou Wang[a], Jin Ye[a], Daojin Li[a], Zhen Liu[a,*] and Xingcai Wu[b,*]

Being confined within nanoscale space, substances may exhibit unique physicochemical properties. The effect of nanoconfinement on molecular interactions is of significance, but a sound understanding has not been established yet. Here we present a quantitative study on boronate affinity (covalent) and electrostatic (non-covalent) interactions confined within mesoporous silica. We show that both interactions were enhanced by the confinement and the enhancement depended on the closeness of the interacting location as well as the difference between the pore size and the molecular size. The overall enhancement could reach 3 orders of magnitude.

As a unique phenomenon, confinement effect has attracted enormous attentions from physics to chemistry to material science. When a substance is confined in a nanoscale space, its physicochemical properties, such as density,[1] miscibility,[2] rigidity,[3] reactivity,[4] catalytic activity,[5] and so on, may be dramatically different from those under non-confined conditions. Nanoconfinement effect often occurs in advanced materials such as nanomaterials,[6] mesoporous materials,[7] porous materials[8] and nanopatterned surfaces.[9] Thus, a comprehensive understanding of nanoconfinement effect can not only enable favorable properties but also facilitate rational design of advanced functional materials.

Molecular interaction is the fundamental of multiple areas, such as sensing, separation, catalysis, drug delivery, and so on. In recent two decades, many advanced functional materials, which may involve in spatial confinement, have found increasing applications. For example, macroporous monoliths have been important media for chromatographic separations[10] while functionalized mesoporous materials have been widely used as effective absorbents for sample pretreatment,[11] and drug delievery.[12] Besides, molecularly imprinted polymers (MIPs),[13] whose specific binding with their targets relies on the 3D shape matching between nanoscale imprinted cavities and targets, have been practical substitutes for antibodies in many applications, while the nanopore of macroporous monolith has been utilized as a core element for the design of biomimetic materials.[14] However, confinement effect on interactions associated with advanced functional materials has never been well studied. Although Himmelhaus et al. reported confinement-induced enhancement of antigen-antibody interactions within nanopatterns[9a] and Wu et al. reported the confinement effect on dipole-dipole interactions in nanofluids,[15] understanding of molecular interactions under confined space has been still very limited.

Herein we present for the first time a quantitative study on the effect of nanoscale confinement on molecular interactions using functionalized mesoporous silica as a host material. We show that both covalent and non-covalent interactions were enhanced by confinement and the enhancement depended on the closeness of the interacting location as well as the difference between the pore size and the molecular size. The more closed the interacting location, the larger the enhancement was; the smaller the difference, the larger the enhancement was. The overall enhancement could reach 3 orders of magnitude. These findings can not only provide new insights into molecular interactions under nanoconfinement but also facilitate rational design of functionalized materials for important applications, such as separation, drug delivery, sample preparation, and so on.In this study, MCM-41-type channel-like mesoporous silica nanoparticle was employed as a model host material because of its unique well-ordered mesoporous structure. 4-Carboxyphenylboronic acid (CPBA) functionalized-MCM-41-type mesoporous silica nanoparticle with an average diameter of 80 nm and a pore diameter of 2.6 nm was used as the main host material to provide spatial confinement, while CPBA-modified nonporous silica sphere with an average diameter of 120 nm was used as a control to yield non-confined environment (Figure S1 in the ESI). The CPBA-functionalized mesoporous silica nanoparticles were prepared according to a literature method.[16] Briefly, bare mesoporous silica nanoparticles were first synthesized; after being amino-functionalized, 4-carboxyphenylboronic acid moieties were then modified onto the pore walls of the mesoporous silica. Nonporous silica nanoparticles were prepared according to a literature method[17] with major modifications, followed by CPBA-functionalization via similar procedure. Three cis-diol-containing molecules with diverse molecular size, including adenosine (276 Da), RNase B (15.5 kDa) and horseradish peroxidase (HRP) (44 kDa), as well as a non-cis-diol containing protein, RNase A (13.5 kDa), were employed as representative guest molecules. Scheme 1 depicts the molecular interactions under different spatially confined conditions in this

study. There were three kinds of chemical moieties at the surface of the mesoporous and nonporous silica: boronic acid, intrinsic silanol and residual amino groups. Under the environmental pH used (pH 8.5), the boronic acid and silanol groups were negatively charged (the pKa values for CPBA and silanol at silica surface were 8.0 and 4.5, respectively) while the amino groups were neutral. Therefore, the guest molecules experienced one or two types of interactions with the host materials: boronate affinity interaction (covalent) or electrostatic attraction/repulsion (non-covalent) or both. According to the location of the interactions, the confinement can be roughly grouped into two classes: 1) full confinement, when the interactions occurred in the interiors of the mesopores; and 2) partial confinement, when the interactions occurred at the boundaries of the mesopores.

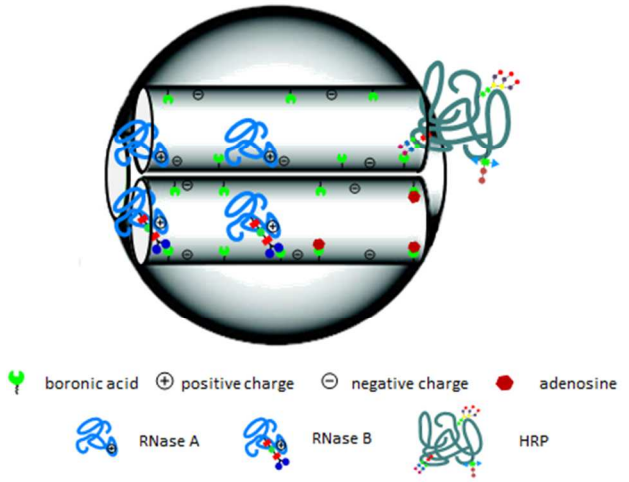

Scheme 1. Schematic of molecular interactions under different spatially confined conditions.

As its pK_b value is 10.5,[18] adenosine was uncharged under pH 8.5 and it only experienced boronate affinity interaction with the ligand. RNase A is a basic nonglycoprotein with isoelectric point (pI) of 9.6, it interacted with CPBA-mesoporous silica nanoparticle solely through electrostatic attraction. RNase B is a basic glycoprotein (pI, 8.9), it interacted with the host materials through boronate affinity interaction and electrostatic attraction. Since RNase A, whose radius of gyration was 1.5 nm,[19] can be encapsulated by mesopores with a diameter of 2.5 nm,[20] it can be expected that RNase A, RNase B (slightly larger than RNase A in size) and adenosine could pass into the mesopores and their interactions could occur in the interiors and at the boundaries of the mesopores. The pI values of HRP used in this study ranged from 4.2 to 7.6.[21] Therefore, it was negatively charged under pH 8.5 and its interactions with the host materials involved in both boronate affinity binding and electrostatic repulsion. Although the whole molecule of HRP could not get into the mesopores due to its larger size (4.0×6.7×11.7 nm),[22] its glycan chains could extrude into the mesopores and interact with the ligands at the boundaries (partially confined).

The on and off status of the two kinds of interactions can be well manipulated by choosing appropriate pH. Boronate affinity interaction is a pH-controlled reversible binding.[23] Boronic acids can covalently react with cis-diols containing compounds to form five- or six-membered cyclic esters in an alkaline aqueous solution (pH ≥ pKa of the boronic acid), while the esters dissociate upon switching the solution to acidic pH (usually < 3.0). The electrostatic attraction for the interacting species in this study also obeys the same pH-controlled on/off pattern, because the boronic acid becomes uncharged at acidic pH. The pH-switchable adsorption/desorption properties ensured the accuracy of binding strength characterization. On the other hand, the electrostatic attraction and repulsion can be suppressed by adding enough salt to the binding environment.

The boronate affinity selectivity of the CPBA-functionalized mesoporous and nonporous silica was confirmed by the selective extraction of adenosine against its non-cis-diol analogue deoxyadenosine (Figure S2 in the ESI). Transmission electron microscopy (TEM) confirmed the expected structures and morphology of CPBA-functionalized mesoporous and nonporous silica (Figure 1A). Digitalization analysis of the TEM images were used to investigate the location of the test molecules (Figure 1B). CPBA-mesoporous silica incubated with adenosine, RNase A, RNase B showed lower normalized pixel intensity than CPBA-mesoporous silica, indicating all these molecules entered the pores. Meanwhile the normalized pixel intensity deceased as increasing the molecular size. Adenosine is the smallest molecule, it experienced the lightest confinement. RNase B is the largest among the three compounds, it experienced the tightest confinement. The normalized pixel intensity for HRP-incubated mesoporous silica was lower than that for RNase B-incubated mesoporous silica. This is attributed to that the HRP molecules covered most of the mesopores, even they were just partially confined. X-ray diffraction (XRD) patterns (Figure 1C), N_2 adsorption/desorption analysis (Fig. S3 in the ESI) and pore size distributions (Fig. S4 in the ESI) for the mesoporous silica alone and incubated with the interacting species all confirmed the presence of mesopores in the mesoporous silica as well as the spatially confined status of the interacting species by the mesopores.

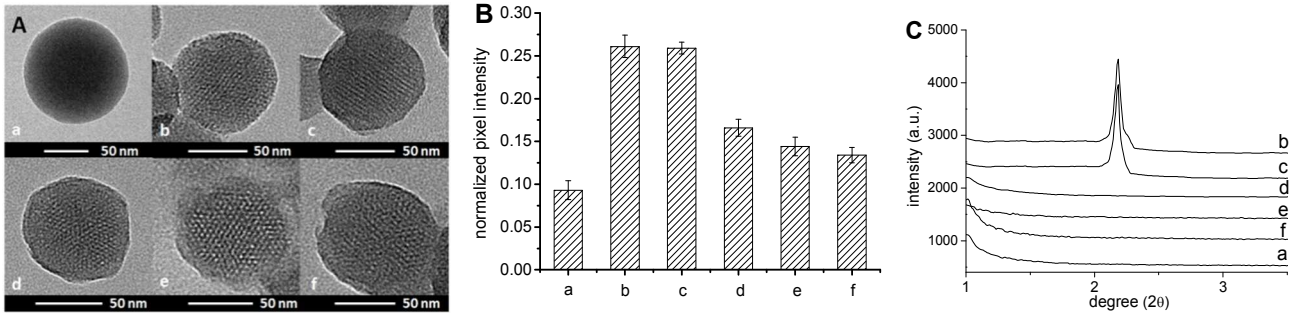

Fig. 1. A) TEM images and B) column graphs of pixel intensity ratio between pore and background in the TEM images and C) XRD patterns for a) CPBA-nonporous silica, b) CPBA-mesoporous silica, c) CPBA-mesoporous silica incubated with adenosine, d) CPBA-mesoporous silica incubated with RNase A, e) CPBA-mesoporous silica incubated with RNase B, and f) CPBA-mesoporous silica incubated with HRP.

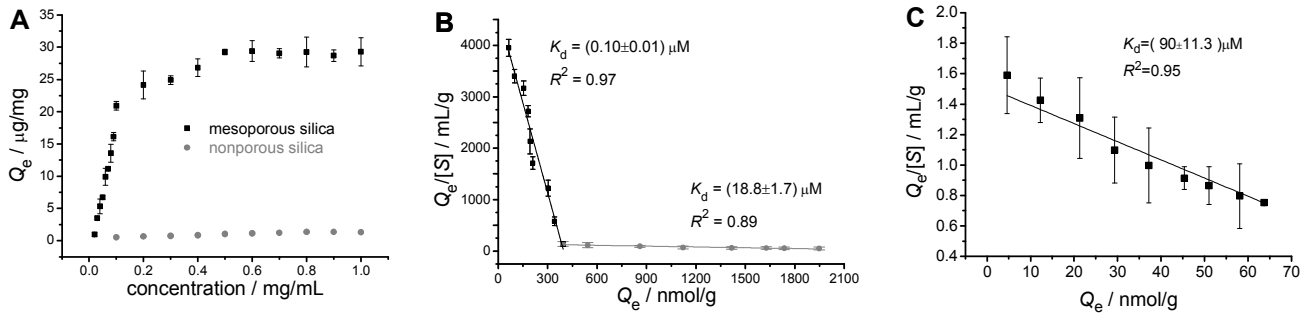

Fig. 2. A) Binding isotherms for the binding of RNase B with CPBA-mesoporous and CPBA-nonporous silica; B) Scatchard plots for the binding of RNase B with CPBA-mesoporous silica; C) Scatchard plots for the binding of RNase B with CPBA-nonporous silica (See the ESI for the definitions of Q_e and [S]).

Table 1. Disassociation constants (K_d) of selected molecules with CPBA-mesoporous and CPBA-nonporous silica[a]

Molecule and its molecular weight	Interaction type	CPBA-mesoporous silica		CPBA-nonporous silica		Enhancement factor
		K_d (μM)	R^2	K_d (μM)	R^2	
Adenosine	BA	710±110	0.98	5300±200	0.98	7.5
(276 Da)		3600±730	0.89			1.5
RNase A (13.7 kDa)	EA	0.9±0.1	0.92	64.1±1.6	0.99	71.1
RNase B[b]	BA	1.4±0.2	0.95	63.3±5.1	0.94	45.2
(15.5 kDa)		10.4±1.3	0.92			6.1
RNase B	BA & EA	0.1±0.01	0.97	90±11.3	0.95	9.0×10^2
(15.5 kDa)		18.8±1.7	0.89			4.8
RNase B[c]	BA & EA	0.043±0.007	0.97			2.1×10^3
(15.5 kDa)		13.7±1.1	0.93			6.6
HRP (44 kDa)	BA & ER	4.3±0.3	0.97	34.6±1.7	0.96	8.0

[a.] the pore size of the CPBA-mesoporous silica: 2.6 nm, unless otherwise specified; the binding buffer: 30 mM phosphate buffer, pH 8.5, unless otherwise specified; BA: boronate affinity interaction; EA: electrostatic attraction; ER: electrostatic repulsion. [b.] the binding buffer: 30 mM phosphate buffer containing 500 mM NaCl, pH 8.5. [c.] the pore size of the CPBA-mesoporous silica: 2.1 nm.

In order to accurately measure dissociation constants (K_d) for the binding between the mesoporous silica and the test proteins, a long equilibrium time (12 h at room temperature) under shaking condition was applied, to ensure equilibria between the free proteins outside of mesoporous silica and the bound proteins inside of mesoporous silica. Fluorescence spectrum test and enzymatic activity test confirmed that no apparent conformational change or denaturation occurred for all the test proteins due to shaking (Fig. S5 in the ESI). Thus, adsorption isotherms for the interactions between the CPBA-mesoporous silica and CPBA-nonporous silica with the four compounds were established and the according dissociation constants (K_d) were measured by Scatchard analysis (a frequently used method for measuring equilibrium constants for reversible ligand/receptor interactions, see Experimental Section and Fig. S6-S9 in the ESI). Table 1 lists the K_d values for the four compounds in 30 mM phosphate buffer (pH 8.5) and for RNase B in 30 mM phosphate buffer containing 500 mM NaCl (pH 8.5). Literature K_d values by surface plasmon resonance (SPR) for binding between phenylboronic acid and glucose (4.9 mM)[24] and ovalbumin (76.9 μM)[25] confirmed the reliability of the method employed in this study. The Scatchard analysis provided not only quantitative characterization of binding strengths but also differentiation of binding locations. The Scatchard plots for the interactions between adenosine and RNase B with CPBA-mesoporous silica exhibited two distinct K_d values. The differences are attributed to the different confinement extents of these molecules in the interiors and at the boundaries of the mesopores. The guest molecules bound in the interiors exhibited lower dissociation constants while those bound at the boundaries exhibited higher dissociation constants. As comparison, the interactions of RNase A and HRP with CPBA-mesoporous silica exhibited only single K_d values. The reason for HRP is easy to understand because it was just partially confined by the mesopores. The reason for RNase A may be more complicated, but the experimental result might suggest that the interactions of RNase A occurred predominantly in the interiors of the mesopores.

Based on the experimental K_d values listed in Table 1, the confinement effect on the interactions at different conditions can be quantitatively examined. Clearly, the binding strengths for all guest molecules were enhanced by the spatial confinement. It is also apparent that both boronate affinity binding and electrostatic interaction were enhanced by the spatial confinement of the mesopores. On one hand, the enhancement of the binding strength noticeably depended on the closeness of the interacting location. At less closed locations (at the boundaries), the binding strengths were slightly improved, by only 1.5-8.0 fold. While at more closed locations (in the interiors), the binding strengths were dramatically enhanced, by 45-900 fold. On the other hand, the enhancement of binding strength strongly depended on the difference between the molecule size and the pore size. The smaller the difference, the larger the enhancement was. For boronate affinity binding under full confinement, the binding strength of adenosine was enhanced by only 7.5-fold while that of RNase B was enhanced by 45.2-fold.

For an interacting host-guest pair that involved multiple interactions, the interplay between the enhancement effects on individual interactions was distinct for different binding locations. For interactions occurring in the interiors of the mesopores, the enhancement effects seemed to be multiplicative. For instance, the sole boronate affinity binding between RNase B and the ligand was enhanced only by 45.2-fold while if electrostatic attraction was also involved, the overall binding strength was enhanced by 900-fold. However, for interactions occurring at the boundaries of the mesopores, the interplay was complicated.

From the above discussion, it can be expected that the binding strength of the interactions occurring in the mesoporous silica can be further enhanced by reducing the size of the mesopore. To confirm such an expectation, CPBA-mesoporous silica with a pore diameter of 2.1 nm was synthesized. When both boronate affinity interaction and electrostatic attraction coexisted, the K_d value for the binding between RNase B and the 2.1-nm mesoporous silica was determined to be 4.3×10^{-8} M (Fig. S10 in the ESI), which is 2100-fold higher than that for non-confined conditions.

In conclusion, we have quantitatively examined how spatial confinement affects molecular interactions. Since two typical interaction types (covalent boronate affinity interaction and non-covalent electrostatic attraction/repulsion) were investigated, enhanced molecular interactions by nanoconfinement can be considered as a general rule. Despite only mesoporous material was investigated, the nanoconfinement effect should be applicable to various materials. The new findings in this study have important implications for not only understanding of molecular interactions under nanoconfinement but also rational design of functionalized materials. On one hand, the nanoconfinement effect can provide rational explanations for enhanced properties of advanced materials. For instance, a recent finding revealed that the binding strength of a boronate affinity-based MIP[12c] toward a target glycoprotein was enhanced by 5 orders of magnitude as compared with the interaction between a comparable boronic acid and the same glycoprotein in solution.[26] This can be attributed to a great extent to the confinement effect of nanoscale imprinted cavities. On the other hand, confinement effect can provide an effective strategy to enhance molecular interactions for the purposes of molecular recognition, separation, drug delivery, and so on. Recently, multivalent synergistic binding has been demonstrated as an strategy that can enhance boronate affinity binding strength by 3-4 orders of magnitude.[27] Obviously, the combination of confinement effect and multivalent synergistic binding will be a supper powerful strategy to fabricate functionalized materials with high binding strength toward specific targets.

Acknowledgements

We acknowledge the financial support of the Key Grant of 973 Program (No. 2013CB911202) from the Ministry of Science and Technology of China, the grants (Nos. 21075063, 21275073 and 21121091) from the National Natural Science Foundation of China, and the general grant (No. KB2011054) from the Natural Science Foundation of Jiangsu Province, China, to ZL.

Notes and references

[a] State Key Laboratory of Analytical Chemistry for Life Science, School of Chemistry and Chemical Engineering, Nanjing University, 22 Hankou Road, Nanjing , 210093, China
Fax: (+86) 25-8368-5639
E-mail: zhenliu@nju.edu.cn
[b] Key Laboratory of Mesoscopic Chemistry of Ministry of Education, School of Chemistry and Chemical Engineering, Nanjing University, 22 Hankou Road, Nanjing, 210093, China
E-mail: wuxingca@nju.edu.cn

†Electronic Supplementary Information (ESI) available: experimental details, characterization data, protein stability test, measurement of adsorption isotherms, data analysis. See DOI: 10.1039/c000000x/

1 M. Heuberger, M. Zach, N.D. Spencer, *Science* 2001, **292**, 905.
2 S. Zhu, Y. Liu, M.H. Rafailovich, J. Sokolov, D. Gersappe, D.A. Winesett, H. Ade, *Nature* 1999, **400**, 49.
3 J. Klein, E. Kumacheva, *Science* 1995, **269**, 816.
4 a) S. Foley, P. Rotureau, S. Pin, G. Baldacchino, J.P. Renault, J.C. Mialocq, *Angew. Chem. Int. Ed.* 2005, **44**, 110; b) R. Gounder, E. Iglesia, *Angew. Chem. Int. Ed.* 2010, **49**, 808.
5 a) Q. Fu, W. X. Li, Y. Yao, H. Liu, H.Y. Su, D. Ma, X.K. Gu, L.Chen, Z. Wang, H. Zhang, B.Wang, X.H. Bao, *Science* 2010, **328**, 1141; b) E. Castillejos, P.-J. Debouttière, L. Roiban, A. Solhy, V. Martinez, Y. Kihn, O. Ersen, K. Philippot, B. Chaudret, P. Serp, *Angew. Chem. Int. Ed.* 2009, **48**, 2529.
6 H. Dosch, *Appl. Surf. Sci*. 2001, **182**, 192.
7 M.K. Kidder, P.F. Britt, Z.T. Zhang, S.Dai, E.W. Hagaman, A.L.Chaffee, A.C. Buchanan, *J. Am. Chem. Soc.* 2005, **127**, 6353.
8 M.V. Wolkin, J. Jorne, P.M. Fauchet, G. Allan, C. Delerue, *Phys. Rev. Lett.* 1999, **82**, 197.
9 a) S. Krishnamoorthy, M. Himmelhaus, *Adv. Mater.* 2008, **20**, 2782; b) M.F. Crommie, C.P. Lutz, D.M. Eigler, *Science* 1993, **262**, 218.
10 F. Svec, J.M. Fréchet, *Science* 1996, **273**, 205.
11 a) R.J. Tian, H. Zhang, M.L. Ye, X.G. Jiang, L.H. Hu, X. Li, X.H. Bao, H.F. Zou, *Angew. Chem. Int. Ed.* 2007, **46**, 962; b) R.J. Tian, L.B. Ren, H.J. Ma, X. Li, L.H. Hu, M.L. Ye, R.A.Wu, Z.J. Tian, Z. Liu, H.F. Zou, *J. Chromatogr. A* 2009, **1216**, 1270; c) Y. Xu, Z. Wu, L. Zhang, H. Lu, P.Y. Yang, P.A. Webley, D.Y. Zhao, *Anal. Chem*. 2009, **81**, 503; d) H. Qin, P. Gao, F. Wang, L. Zhao, J. Zhu, A. Wang, T. Zhang, R.A. Wu, H.F. Zou, *Angew. Chem. Int. Ed.* 2011, **50**, 12218.

12 a) K. C.-W. Wu, Y. Yamauchi, *J. Mater. Chem*. 2012*,* **22***,* 1251; b) K. C.-W. Wu, Y. Yamauchi , C.Y. Hong , Y.H. Yang , Y.H. Liang , T. Funatsu, M. Tsunoda, *Chem. Commun*. 2011*,* **47***,* 5232; c) Y.D. Chiang, H.Y. Lian, S.Y. Leo, S.G. Wang, Y. Yamauchi, K. C.-W. Wu*, J. Phys. Chem. C,* 2011*,* **115***,* 13158.
13 a) G. Vlatakis, L.I. Andersson, R. Muller, K. Mosbach, *Nature* 1993, **361**, 645. b) H. Shi, W.B. Tsai, M.D. Garrison, S. Ferrari, B.D. Ratner, *Nature* 1999, **398**, 593; c) L. Li, Y. Lu, Z.J. Bie, H.Y. Chen, Z. Liu, *Angew. Chem. Int. Ed.* 2013, **52**, 7451; d) S.S. Wang, J. Ye, Z.J. Bie, Z. Liu, *Chem. Sci.* 2014, **5**, 1135.
14 Y.C. Liu, Y. Lu, Z. Liu, *Chem. Sci.* 2012, **3**, 1467.
15 J. Baugh, A. Kleinhammes, D.X. Han, Q. Wang, Y. Wu, *Science* 2001, **294**, 1505.
16 Zhao, Y.N, Trewyn, B.G, Slowing, I.I, Lin, V.S.-Y. *J. Am. Chem. Soc.* 2009**, 131,** 8398.
17 Chang, S. M.; Lee, M.; Kim, W.-S. *J. Col. Interf. Sci.* 2005, **286**, 536
18 G.W. Muth, L. Ortoleva-Donnelly, S.A. Strobel, *Science* 2000, **289**, 947.
19 G. Panick, R. Winter, *Biochem*. 2000, **39**, 1862.
20 R. Ravindra, Z. Shuang, H. Gies, R. Winter, *J. Am. Chem. Soc.* 2004, **126**, 12224.
21 P. Dou, Z. Liu, *Anal. Bioanal. Chem*. 2011, **399**, 3423.
22 G.I. Berglund, G.H. Carlsson, A.T. Smith, H. Szoke, A. Henriksen, J. Hajdu, *Nature* 2002, **417**, 463.
23 a) R. Nishiyabu, Y. Kubo, T.D. James, J.S. Fossey, *Chem. Commun*. 2011, **47**, 1106; b) R. Nishiyabu, Y. Kubo, T.D. James, J.S. Fossey, *Chem. Commun*. 2011, **47**, 1124; c) G. Springsteen, B.H. Wang, *Tetrahedron* 2002, **58**, 5291; d) L.B. Ren, Z. Liu, Y.C. Liu, P. Dou, H.Y. Chen, *Angew. Chem. Int. Ed*. 2009, **48**, 6704; e) L. Liang, Z. Liu, *Chem. Commun.* 2011, **47**, 2255; f) H.Y. Li, Z. Liu, *Trac-Trend Anal. Chem*. 2012, **37**, 148; g) H.Y. Nie, Y. Chen, C.C. Lü, Z. Liu, *Anal. Chem.* 2013, **85**, 8277.
24 A. Stephenson-Brown, H.C. Wang, P. Iqbal, J.A. Preece, Y.T Long, J.S. Fossey, T.D. James, P. M. Mendes, *Analyst*, 2013, **138**, 7140
25 H. Kitano, Y. Anraku, H. Shinohara, *Biomacromolecules* 2006, **7**, 1065.
26 C.C. Lü, H.Y. Li, H.Y. Wang, Z. Liu, *Anal. Chem.* 2013, **85**, 2361.
27 H.Y. Wang, Z.J. Bie, C.C. Lü, Z. Liu, *Chem. Sci.* 2013, **4**, 4298.